MNRAS **443,** 2801–2814 (2014) doi:10.1093/mnras/stu1321

Stochastic angular momentum slews and flips and their effect on discs in galaxy formation models

Nelson D. Padilla,[1,2⋆] Salvador Salazar-Albornoz,[1,3,4] Sergio Contreras,[1] Sofía A. Cora[5,6,7] and Andrés N. Ruiz[7,8,9]

[1] *Instituto de Astrofísica, Pontificia Universidad Católica de Chile, Santiago, Chile*
[2] *Centro de Astro-Ingeniería, Pontificia Universidad Católica de Chile, Santiago, Chile*
[3] *Universitäts-Sternwarte München, Scheinerstrasse 1, D-81679 Munich, Germany*
[4] *Max-Planck-Institut für extraterrestrische Physik, Giessenbachstrasse 1, D-85748 Garching, Germany*
[5] *Instituto de Astrofísica de La Plata (CCT La Plata, CONICET, UNLP), Paseo del Bosque s/n, B1900FWA, La Plata, Argentina*
[6] *Facultad de Ciencias Astronómicas y Geofísicas, Universidad Nacional de La Plata, Paseo del Bosque s/n, B1900FWA, La Plata, Argentina*
[7] *Consejo Nacional de Investigaciones Científicas y Técnicas, Rivadavia 1917, Buenos Aires, Argentina*
[8] *Instituto de Astronomía Teórica y Experimental (CCT Córdoba, CONICET, UNC), Laprida 854, Córdoba, X5000BGR, Argentina*
[9] *Observatorio Astronómico de Córdoba, Universidad Nacional de Córdoba, Laprida 854, Córdoba, X5000BGR, Argentina*

Accepted 2014 July 2. Received 2014 June 6; in original form 2013 September 4

ABSTRACT

The angular momentum of galactic discs in semi-analytic models of galaxy formation is usually updated in time as material is accreted to the disc by adopting a constant dimensionless spin parameter and little attention is paid to the effects of accretion with misaligned angular momenta. These effects are the subject of this paper, where we adopt a Monte Carlo simulation for the changes in the direction of the angular momentum of a galaxy disc as it accretes matter based on accurate measurements from dark-matter haloes in the Millennium II simulation. In our semi-analytic model implementation, the flips seen in the dark-matter haloes are assumed to be the same for the cold baryons; however, we also assume that in the latter the flip also entails a difficulty for the disc to increase its angular momentum which causes the disc to become smaller relative to a no-flip case. This makes star formation to occur faster, especially in low-mass galaxies at all redshifts allowing galaxies to reach higher stellar masses faster. We adopt a new condition for the triggering of starbursts during mergers. As these produce the largest flips it is natural to adopt the disc instability criterion to evaluate the triggering of bursts in mergers instead of one based on mass ratios as in the original model. The new implementation reduces the average lifetimes of discs by a factor of $\sim$2, while still allowing old ages for the present-day discs of large spiral galaxies. It also provides a faster decline of star formation in massive galaxies and a better fit to the bright end of the luminosity function at $z = 0$.

Key words: galaxies: evolution – galaxies: fundamental parameters – galaxies: general – galaxies: structure.

1 INTRODUCTION

The formation and evolution of galactic discs in a universe dominated by dark matter poses great challenges that still need to be solved. For instance, only recently grand design discs such as that of the Milky Way have been produced in hydrodynamical simulations with a better treatment of multiple gas phases and feedback (Scannapieco et al. 2006) and with the hybrid lagrangian cell code AREPO (Springel 2010). On the other hand, it is difficult to produce large enough samples of galaxies with these codes to make statistical comparisons with galaxy samples extracted from large surveys such as the Sloan Digital Survey (York et al. 2000) due to the large computational resources required for this in comparison to simulations that only follow dark matter (see e.g. Bower, Benson & Crain 2012).

In recent years, these problems have been partially solved by different approaches such as (i) using resimulations of chosen haloes in large dark-matter only simulations to much higher resolutions, as is the case of the Aquarius simulations (Springel et al. 2008). These

⋆ E-mail: npadilla@astro.puc.cl

haloes resemble our own Milky Ways (MW), and simulations of galaxies within these are expected to reproduce the large disc of the MW at least in some cases. These simulations have been extensively analysed and different hydrodynamical codes have been run using the Aquarius simulations (the Aquila project; Scannapieco et al. 2012), and in some cases their results are promising showing grand-design spiral galaxies in a fraction of the haloes (Marinacci, Pakmor & Springel 2014). (ii) Resimulating larger portions of the Millennium Simulation (Springel et al. 2005) corresponding to different environments, of low, average and high matter density; this is the case of the GIMIC project (Galaxies-Intergalactic medium Interaction Calculation; Crain et al. 2009). However, it turned out that the resulting stellar mass function of the GIMIC galaxy population is not compatible with the observed one (Bower et al. 2012). The limitation of this approach is evident since due to the high computational demand of this project, it was not possible to re-run it many times with changing parameters until the resulting galaxy population matched the observed one. (iii) Currently, the EAGLE project (Evolution of Galaxies and their Environment; Bower et al. 2012) seems the most promising way to obtain fully hydrodynamical simulations of a galaxy population with the right stellar mass function, that is, with a reasonable galaxy population in which each galaxy has evolved embedded in a dark-matter halo, with all the associated physical effects, including those involved in the formation and evolution of galactic discs.

Still, even though cosmological volumes are being simulated using reasonable hydrodynamics, in some cases there are still issues regarding the resulting efficiency of early star formation, which can be higher than observed (e.g. Nagamine 2010; Brook et al. 2011; Powell, Slyz & Devriendt 2011, and references therein). The proposed solution to this appears to come from adopting higher resolution and introducing additional sources of feedback (e.g. Hopkins, Quataert & Murray 2011; Tasker 2011; Kannan et al. 2014).

Another solution to the problem of making large galaxy samples from simulations comes from semi-analytic models of galaxy formation. These models are necessarily extremely simplified versions of the hydro simulations, since a small set of simple equations describes the evolution of, for instance, an entire gas phase in a galaxy (Kauffmann et al. 1999; Cole et al. 2000, see also the reviews by Baugh 2006; Benson 2010; Silk & Mammon 2012); this is, however, the reason why it is feasible to generate large galaxy populations with these models. In particular, the process of star formation is generally modelled according to the observed proportionality between star formation rate and projected gas density (e.g. Kennicutt 1998). The proportionality constant involves an efficiency parameter, which is fixed so as to fit the observed $z = 0$ galaxy luminosity function, among other properties. Notice that the early over-efficiency of star formation affecting some hydrodynamical simulations is therefore not present in semi-analytic models, since they directly fix the efficiency of star formation by reproducing the observed total mass in stars at $z = 0$.

The ingredients involved in the star formation process in semi-analytics are the disc dynamical time and the mass of cold gas contained in the disc (e.g. Cole et al. 2000; Croton et al. 2006; Lagos, Cora & Padilla 2008, among others). Of the two, the dynamical time is the most delicate in the sense that it depends strongly on the size of the disc, and this is a challenging quantity as it involves many complicated evolutionary processes. For instance, we need to know the angular momentum of the disc and the influence of the bulge in its final size. Practical answers to these questions were given by Mo, Mao & White (1998, hereafter MMW), by studying the behaviour of discs in numerical simulations. For relaxed haloes, they were able to provide formulae for the typical disc size that depend on the dark-matter halo mass, its specific angular momentum, λ, the fraction of mass residing in the disc, and the fraction of mass in the bulge.

However, haloes acquire mass continuously, either in a smooth way or via mergers, and in both cases, the angular momentum of the halo suffers slews and flips, some of them small but others as high as 90° or even more. Bett & Frenk (2012) studied the frequency of flips in dark-matter only simulations. They showed that flips are more likely in mergers, but that they still occur when there is smooth accretion. If the hot gas is relaxed within the dark-matter halo, as it cools it is highly likely that the disc sitting in the centre will have a different angular momentum. Analysing the GIMIC galaxies, Sales et al. (2012) showed that this effect can destroy discs completely, making their life more episodic than is usually obtained in semi-analytic models, where unless a merger or a disc instability (DI) takes place, the disc keeps growing (on average). In the same line, Aumer et al. (2013) find that the last misaligned accretion influences the disc fraction of a galaxy. Other studies of disc galaxies show the complex physics of discs. Saha & Naab (2013) find that the alignment of the angular momentum direction of the disc and halo produce stronger bars, which in principle could suggest that not even aligned discs are guaranteed to survive long. In a more cautious note, Bird et al. (2013) analysed the Eris ensemble of resimulated haloes (Guedes et al. 2011), and point out that initial conditions have an important influence on the final state of the disc of a galaxy.

The aim of this paper is to evaluate the impact on the properties of galactic discs of the angular momentum slews and flips suffered by dark-matter haloes using the semi-analytic model of galaxy formation SAG (Cora 2006; Lagos et al. 2008; Lagos, Padilla & Cora 2009a; Tecce et al. 2010). Although the version of the model described in Tecce et al. (2010), to which we will refer to as the base model, makes full use of the MMW formulae to determine disc sizes, it does not take into account the change of the angular momentum of the discs as they accrete matter. In this paper we will improve upon this recipe by taking this effect into account, to some degree, developing a new version of this model that we will refer to as the flip model. For this purpose, we construct a statistics of angular momentum slews using the Millennium II simulation (Boylan-Kolchin et al. 2009) and, with the aid of a Monte Carlo simulation, apply slews in the discs of the semi-analytic galaxies. The resulting properties of galactic discs impact directly the frequency of DI events suffered by a galaxy, in which the disc is transferred to the galactic bulge with all the cold gas available being consumed in a starburst. The chance of bursts increases with the amplitude of the flip of the angular momentum of the discs, which makes us implement one additional modification to our model regarding the triggering of starbursts during galaxy mergers. Instead of using mass ratios of the merging galaxies to classify them as major mergers with starburst or minor mergers with and without starbursts, as is considered in the base model, we now apply the DI criterion to the remnant galaxy.

One of the possible consequences of introducing angular momentum flips in galaxy discs in the model is that it could affect the rate at which star formation occurs at high redshift. Since a few years back there has been some tension between the observed abundance of massive galaxies at high redshift and those predicted by semi-analytic models (e.g. de Lucia et al. 2006). Several observational studies pointed at larger populations of high stellar mass galaxies than predicted (e.g. Pérez-González et al. 2008; Ferreras et al. 2009), but with the advent of mid-infrared imaging of high

redshift galaxies, this situation was somewhat alleviated, as shown by Marchesini et al. (2010). They point out that if dusty templates are included in the analysis of photometric samples of galaxies with mid-IR coverage, then the tension with the models is reduced. With an increased star formation activity at high redshifts, our new model could help to reduce even further this controversy.

This paper is organized as follows. In Section 2 we present the statistics on angular momentum slews extracted from the Millennium II simulation (Boylan-Kolchin et al. 2009), and we briefly describe the aspects of the semi-analytic model relevant to the present study and the improvements introduced regarding the slews of dark-matter angular momentum; Section 3 shows the effects of these specific changes on the typical lifetimes of discs in galaxies. Section 4 shows how with this new model we can follow bursts in mergers using only the DI criterion instead of mass ratios as in the base model. In Section 5 we explore the consequences of this new treatment on the general properties of the model galaxy population, and Section 6 summarizes our results.

2 ANGULAR MOMENTUM SLEWS AND FLIPS IN A SEMI-ANALYTIC MODEL

We use the SAG (Semi-Analytic Galaxies) semi-analytic model of galaxy formation which is based on the one described by Springel et al. (2001), with improvements on the chemical element production by Cora (2006), the implementation of active galactic nucleus (AGN) feedback in Lagos et al. (2008), and the inclusion of MMW disc sizes by Tecce et al. (2010). SAG is run on subhalo merger trees extracted from a dark-matter only N-body simulation. This simulation is based on the standard ΛCDM scenario, characterized by the cosmological parameters $\Omega_{\rm m} = 0.28$, $\Omega_{\rm b} = 0.046$, $\Omega_\Lambda = 0.72$, $h = 0.7$, $n = 0.96$, $\sigma_8 = 0.82$, according to the *WMAP*7 cosmology (Jarosik et al. 2011). The simulation was run using GADGET-2 (Springel 2005) using 640^3 particles in a cubic box of comoving sidelength $L = 150\,h^{-1}$ Mpc.

In this paper, we introduce angular momentum slews and flips that will directly affect the galaxy discs. One simple way to do this is to follow the angular momentum vector of the dark-matter halo which changes with time, and assume that the hot gas always carries it, even when cooling down to top up the cold gas supply of the disc. The incoming cold gas brings angular momentum parallel to that of the halo, but if the halo changed its spin with respect to the time when the disc was formed, the cooling gas will have a different angular momentum than the disc. Using mass weighted averages of the angular momenta of the incoming cold gas and the galaxy disc, Lagos et al. (2009a) followed the changes in the angular momentum of the galaxy disc. They went even further and extended this to the spin of the black hole (see also Guo et al. 2011; Lagos et al. 2011).

However, the direction of the angular momentum of haloes is difficult to measure accurately; for haloes with less than 1000 particles the direction is subject to large contributions from numerical noise (e.g. Bett & Frenk 2012). Therefore, the changes in the direction of the angular momentum of haloes in this case are larger than it would be if the haloes were followed with higher resolution. In our case, therefore, we either need to smooth this effect to some degree (as was done in Lagos et al. 2009a), or use a statistical measurement of the typical angular momentum flips of haloes to apply it to a semi-analytic model.

We opt for the latter, for which the first step is to obtain a full statistical distribution of flips from a numerical simulation with enough resolution so that the full dynamical range of haloes populated by SAG is covered by our statistics. The Millennium II simulation (Boylan-Kolchin et al. 2009) provides us with subhaloes of $M > 10^{10}\,h^{-1}\,{\rm M}_\odot$ with more than 1000 particles each, fulfilling this requirement (Lemson et al. 2006).[1]

We will use subhaloes instead of haloes from the start, to avoid the influence in the measured angular momentum from other substructures. This way satellites will slew according to the angular momentum of their host substructures and not of their host halo as a whole. Furthermore, central galaxies are this way unaffected by the changes in the angular momentum of their satellites, which should not contribute to the central galaxy's angular momentum until the event of a merger.

Fig. 1 shows the probability distributions for the cosine of the angle between the initial and final angular momentum ($\alpha_{\rm flip}$) of subhaloes that suffer changes in their mass by the relative amount indicated in the key (these relative mass ranges are chosen as examples, the actual statistics cover a wide range of mass accretion ranging up to $\Delta M/M > 0.5$). These angular momentum changes are commonly referred to as slews or flips. Different line types correspond to whether the increase in mass was by a merger (dashed lines) or smooth accretion (solid lines). The statistics for smooth accretion are obtained analysing subhaloes that have not suffered mergers in consecutive snapshots of the simulation. To construct this for the case of mergers, we take only subhaloes that are the result of at least one merger since the previous snapshot and measure their flips. In the case when the merged subhalo mass is larger than the sum of its progenitor masses, we assume that the excess mass came from smooth accretion. In this case we lower the amplitude of the flip from mergers using the statistics for smooth accretion which are measured first. Only after this correction is made we use it for the statistics of mergers. The upper solid (dashed) line indicates that a higher relative mass accretion (merger) increases the chances of a given angular momentum flip. The upper panel corresponds to low redshifts, $0 < z < 1$, whereas the lower panel to $1 < z < 5$, and as can be seen, the chance of angular momentum flips is higher at higher redshifts.

2.1 Episodic discs

Our application of the probability of slews and flips as a way to follow the evolution of the angular momentum of semi-analytic galaxy discs is simple. In each snapshot of the simulation, we calculate the fractional increase in the galaxy disc mass. We then assign a disc angular momentum flip following the statistical distributions measured from the Millennium II subhaloes, assuming that the same slews or flips are suffered by the baryons in their centres.

However, the most important assumption is that when the disc suffers a flip that amounts to an angle $\alpha_{\rm flip}$, between the 'old' and 'new' angular momenta, this lowers the specific angular momentum of the disc by the following amount:

$$\lambda_{\rm disc} = \lambda_{\rm disc,old}\cos(\alpha_{\rm flip}). \quad (1)$$

The angle $\alpha_{\rm flip}$ accumulates successive slews suffered by an individual disc in a statistical way. As a result, the specific angular momentum of the disc is generally lower than that of the halo at the time the disc formed, and continues to decrease its value as more accretion takes place. This is qualitatively consistent with recent findings that point to lower specific angular momentum for galaxies

[1] The Millennium II simulation data were obtained using the German Astrophysical Virtual Observatory GAVO, at http://gavo.mpa-garching.mpg.de/MyMillennium/

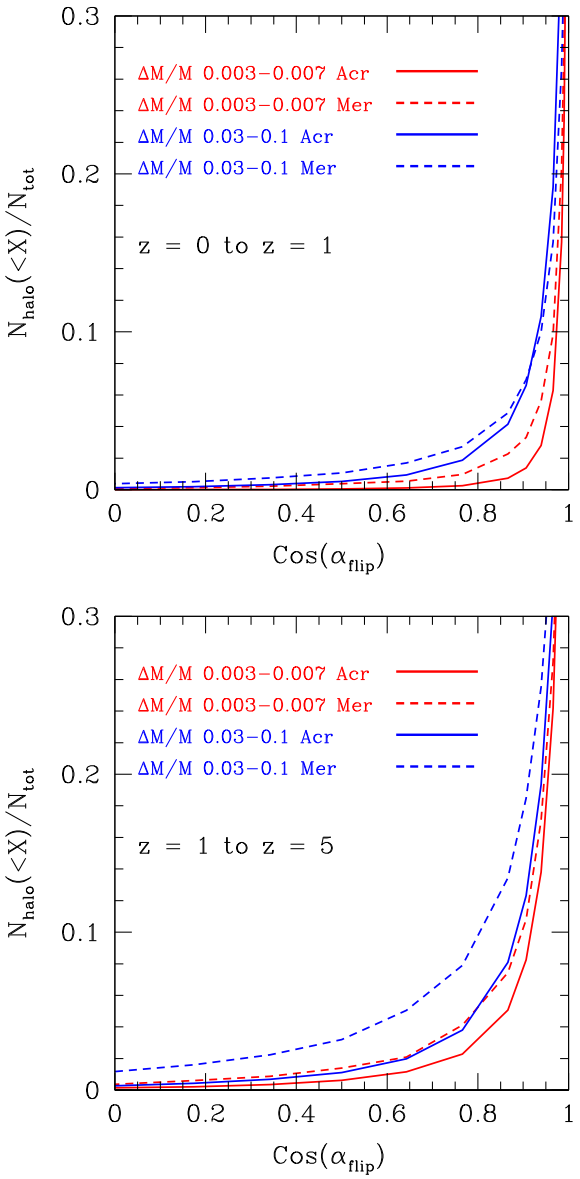

Figure 1. Cumulative distributions of the cosine of $\alpha_{\rm flip}$, the angle between the angular momenta of a dark-matter substructure in the Millennium II simulation before and after accreting matter; these angular momentum changes are commonly referred to as slews or flips. Top and bottom panels correspond to accretion events between $0 < z < 1$ and $1 < z < 5$, respectively. Dashed lines show the distribution of flips in merger events, whereas solid lines are for accretion of individual dark-matter particles. The different colours correspond to two different representative ranges in relative mass accretion, corresponding to $0.003 < \Delta M/M < 0.007$ and $0.03 < \Delta M/M < 0.1$, as indicated in the figure key.

in comparison to that of dark-matter haloes (e.g. Dutton & van den Bosch 2012).

Hydrodynamical simulations and semi-analytic models suffer from opposite problems. It has been pointed out that there is a lack of enough angular momentum to form discs in hydrodynamical simulations (e.g. Mo et al. 1998; Bullock et al. 2001). Recently, Robertson et al. (2006) showed that this can be overcome in cosmological scenarios by taking into account the effect of early merging and appropriate feedback mechanisms (see also Maller & Dekel 2002; Vitvitska et al. 2002; D'Onghia & Burkert 2004). On the other hand, these problems are the opposite in semi-analytic models, where it is usually assumed that the specific angular momentum of the disc equals (e.g. Tecce et al. 2010) or is even higher than that of the dark-matter halo (Berry et al. 2014). This is done because the prescriptions used in these models are not able to follow any of the details of angular momentum and feedback energy transfer. By assuming these equalities, semi-analytic models adopt constant specific angular momenta for discs. However, several works analysing hydrodynamical simulations (Sales et al. 2012; Aumer et al. 2013; Saha & Naab 2013) find that the infall of misaligned material tends to disfavour the survival of the disc whose destruction could be the result of a change in the properties of the disc such as its spin.

Our proposed loss of specific angular momentum of discs is designed to take this effect into account to some degree, as it entails an inhibition of growth of the disc angular momentum due to slews and flips. The initial specific angular momentum of a disc is exactly that of its host halo as it forms, $\lambda_{\rm disc,\,ini}$. Afterward, successive accretion events make the specific angular momentum, $\lambda_{\rm disc}$, smaller with respect to its initial value (without necessarily making the disc actually lose angular momentum). We define

$$\eta_{\rm disc} = \lambda_{\rm disc}/\lambda_{\rm disc,ini}. \quad (2)$$

The value of $\eta_{\rm disc}$ diminishes with each accretion event, but in the case of a merger induced burst of star formation or DI, the disc disappears and, therefore, $\eta_{\rm disc}$ is reset to 1. Only after one halo dynamical time has passed the value of $\eta_{\rm disc}$ is allowed to vary again. We remark that in this implementation we do not follow the changes in amplitude of λ suffered by the host dark-matter structure; we only use its value as a new disc forms as in Cora (2006) and Lagos et al. (2008). As Guo et al. (2011) pointed out, if the disc follows the changes of the specific angular momentum of the dark matter its properties will suffer sudden jumps due to the numerical errors in determining this quantity using few dark-matter particles. We also point out that on average the galaxy population will show a smoothly raising amplitude of angular momentum of discs, but the effect of the slews and flips on the discs specific angular momentum will change its rate of growth.

Notice that even though the amplitude of the dimensionless spin parameter of a disc diminishes, the disc itself slews the direction around which it is spinning by an angle given by the flips distribution measured for the dark matter. This allows us to reproduce, qualitatively, previous well-known results where discs show changes (sometimes important ones) in their direction of spin as a result of mass accretion (e.g. Shen & Sellwood 2006). Also, as is shown in Fig. 1, the distribution of the cosine of angle of flips/slews indicates that an accretion of equal relative mass produces small slews more frequently than actual angular momentum flips. We also note that our formalism does not directly take into account the changes of angular momentum of discs due to external torques which can produce tell tale signs in discs such as warps (e.g. Garcia-Ruiz, Kuijken & Dubinski 2002; Dubinski & Chakrabarty 2009), but these processes do not often entail a loss of angular momentum and, therefore, to first order, do not need to be included in our modelling. Another point to note is that we treat the gas disc as a single object and do not take into account its possible interaction with the stellar disc, or the existence of counter-rotating stars, or stellar warps and other features in the distribution of stars (Bois et al. 2011; Naab et al. 2013; Algorry et al. 2014). Our modelling should include this mechanism for angular momentum transfer between gas and stars, but its effect should be smaller than that coming from the much more frequent accretion events (e.g. Algorry et al. 2014) and we therefore defer its treatment to future work.

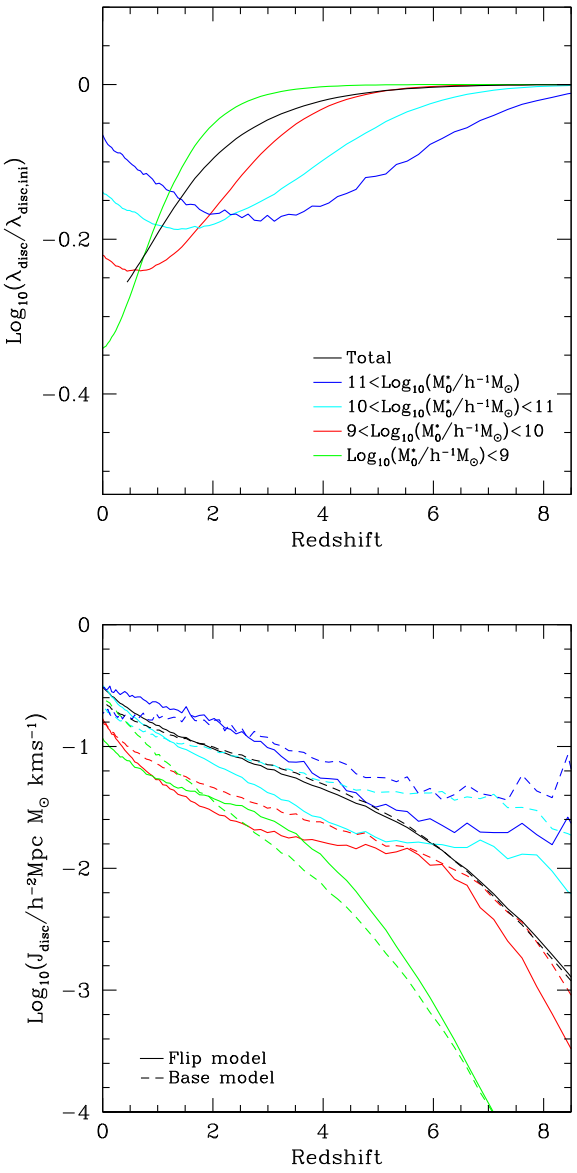

Figure 2. Top: average $\eta_{\rm disc}$ values as a function of redshift for galaxies with present-day stellar masses in four different ranges, as shown by the different colours indicated in the figure key. Bottom: average angular momentum of galaxy discs as a function of redshift, for the same present-day stellar mass ranges as the top panel (different colours), for the base and flip model shown as dashed and solid lines, respectively.

The main motivation behind our implementation comes from the results from hydrodynamical simulations that show that the presence of a disc in a galaxy is favoured by a lack of infall of material coming with a misaligned angular momentum (e.g. Sales et al. 2012; Aumer et al. 2013; Saha & Naab 2013).

Fig. 2 shows the change in the value of $\eta_{\rm disc}$ as a function of redshift for galaxies of different present-day stellar masses, as indicated in the key. As can be seen, more massive galaxies today are tending to $\eta_{\rm disc} = 1$ values, since their evolution consists of a decreasing number of important accretion events. However, at high redshifts, when their masses were still low, their $\eta_{\rm disc}$ reached values as low as 0.65. Notice that less massive galaxies (present-day) climb out of this minimum value of $\eta_{\rm disc}$ at lower redshifts, once they achieve a certain pivot mass. As a consequence of this, the galaxies that today have the lowest $\eta_{\rm disc}$ values are the least massive ones.

The lower panel of the figure shows the evolution with redshift of the average angular momentum of the disc for the base and flip model (dashed and solid lines), for the same ranges of present-day stellar masses as in the top panel. As can be seen, the dips in $\eta_{\rm disc}$ that mark the epoch of large flips correspond to the time when the angular momenta slow their rate of growth, as is the case for the highest present-day stellar masses probed down to $z = 6$; Afterward $\eta_{\rm disc}$ reaches its minimum value and rapidly increases back to unity and the angular momentum grows again. As can be seen, the angular momentum of discs in the base model is usually higher than that in the flip model once the galaxies enter their large flips eras. Stewart et al. (2013) use hydrodynamic simulations to study the evolution of the angular momentum of the gas in individual disc galaxies; in their fig. 2, it can be seen that there are several instances where the angular momentum of the gas grows more slowly than that of the dark matter, and this is the effect that we are reproducing with our simple implementation for the semi-analytic model. Regarding observational results, it is interesting to note that at $z = 0$ only the flip model manages to produce galaxies with higher angular momenta for higher stellar masses, in qualitative agreement with the results of Romanowsky & Fall (2012).

Our assumptions have a number of consequences for the two different cases corresponding to (i) accretion of gas cooling from the hot phase, and (ii) mergers.

In the first case, when the increase in mass is due to accretion of cool gas, the radius of the disc, $r_{\rm disc}$, is impeded from growing and, relative to the no-flip model, becomes slightly smaller as a result of the drop in its dimensionless spin parameter by

$$r_{\rm disc} = \eta_{\rm disc}\, r_{\rm disc,noflip}. \tag{3}$$

This immediately translates into a smaller dynamical time-scale for the disc with respect to the no-flip model, $t_{\rm dyn,\,disc} = r_{\rm disc}/V_{\rm vir}$, where $V_{\rm vir}$ is the subhalo virial velocity, and a higher surface density of gas in the disc, which has a strong impact on the star formation rate of the galaxy, since the model follows the star formation law given by Croton et al. (2006),

$$\dot{m}_* = \alpha_{\rm SF}(m_{\rm cold} - m_{\rm crit})/t_{\rm dyn,disc}, \tag{4}$$

where $\alpha_{\rm SF}$ is the efficiency of star formation, a free parameter of the model, and $m_{\rm crit}$ is the critical mass for star formation given by

$$m_{\rm crit} = 3.8 \times 10^9 \left(\frac{V_{\rm vir}}{200\ {\rm km\ s^{-1}}}\right)\left(\frac{r_{\rm disc}}{10\ {\rm kpc}}\right)\ {\rm M}_\odot. \tag{5}$$

As a result, a flip that impedes the growth of the disc size increases the surface density of gas in the disc, which in turn lowers the critical mass for star formation. This implies that galaxies with flips form more stars (at least for equal star formation efficiency parameters). We adopt a Salpeter initial mass function for all star formation events in the model.

Our model allows for bursts during DIs and mergers. A galaxy becomes unstable when the quantity

$$\epsilon_{\rm d} \equiv \frac{V_{\rm max}}{(GM_{\rm disc}/r_{\rm disc})^{1/2}} \tag{6}$$

is smaller than a critical value of 1. Here, G is the universal gravitational constant and $V_{\rm max}$ is the maximum circular velocity of the disc. We require the effect of a perturbing galaxy as a necessary condition to trigger the DI. When a neighbour galaxy perturbs the unstable disc, all the stars and cold gas in the disc are transferred to the bulge, and this cold gas is consumed in a starburst. A perturbation triggers a starburst only when the typical distance to the galaxies sharing the dark-matter halo of the unstable one is smaller than $d_{\rm pert}$

times the scale-length of the unstable galaxy. Smaller galaxy discs are characterized by lower values of $\epsilon_{\rm d}$. They will therefore tend to produce more frequent instability events, i.e. more frequent bursts of star formation as is seen to occur in hydrodynamical simulations (Sales et al. 2012). They will also tend to produce shorter lived, episodic discs. Additionally, due to the resolution of the Millennium II simulation used to construct the look up tables of slews and flips, the value of $\eta_{\rm disc}$ shows an attractor at small values for a small fraction of the population. Therefore, whenever the condition $\eta_{\rm disc} < 0.1$ is satisfied, we also trigger a burst of star formation as in the case of DIs.

The second case is when the accretion is due to a merger. In the new implementation, we do not apply the rules for merger driven starbursts following ratios of mass between intervening galaxies as in other semi-analytic models, or the previous versions of this one (e.g. Cole et al. 2000; Cora 2006; Lagos et al. 2008; Tecce et al. 2010). We just allow the large flips produced by mergers to produce highly dense discs, which naturally become unstable and undergo bursts. This is an important change introduced in the current version of this semi-analytic model.

2.2 Base model and flip model: comparison of general galaxy properties

The implementation of slews and flips that change the sizes of galaxy discs and the different criterion adopted to allow starbursts during mergers will make for a different galaxy population with respect to the base model. In order to ensure that these differences come only from the new implementation, we will use the same set of model parameters for both models.

We tune the free parameters using the base model. We allow to vary the star formation efficiency $\alpha_{\rm SF}$, the efficiency of supernovae feedback ϵ, the efficiencies of black hole growth during bursts (mergers and DIs) and gas cooling, which are given by $f_{\rm BH}$ and $k_{\rm AGN}$, respectively (see Lagos et al. 2008, for further details), and the parameter $d_{\rm pert}$ involved in the condition for a perturber galaxy to trigger a starburst in an unstable galaxy. This calibration is done via the Particle Swarm Optimization (PSO) search method (presented in Ruiz et al. 2013), using the local galaxy luminosity function in the b_J and K bands, and the relationship between black hole mass and bulge mass as observational constraints. Table 1 presents the free parameters and their best-fitting values found with the PSO technique for the base model.

Differences between the models are expected as in the flip case a higher star formation rate should be produced due to the lower average specific angular momentum of discs resulting from the flips. Additionally, there will probably be a larger number of triggered DIs (cf. Fig. 4) and this, in turn, could provide more material for black hole growth during bursts. Another expected effect is the increase in supernovae feedback which could influence the abundance of dwarf galaxies. These processes, however, are deeply intertwined.

Table 1. Best-fitting parameters found with the PSO technique for the base model.

Parameter	Value
$\alpha_{\rm SF}$	0.20
ϵ	0.25
$f_{\rm BH}$	0.026
$\kappa_{\rm AGN}$	1.4×10^{-3}
$d_{\rm pert}$	21.8

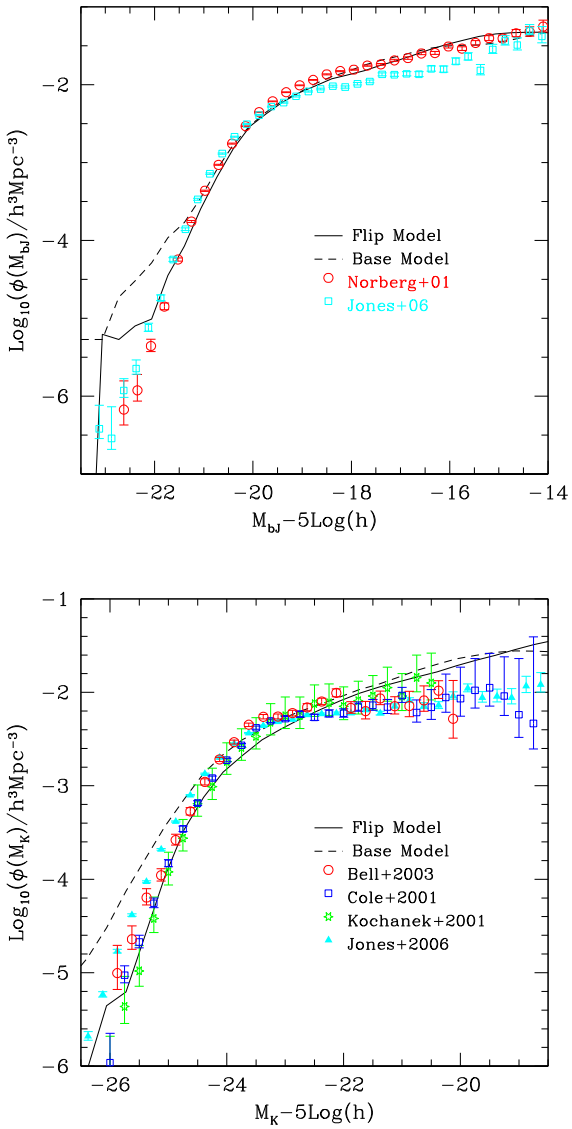

Figure 3. Galaxy luminosity functions in the b_J and K bands (top and bottom panels, respectively), which are the most important of the statistics used in the calibration of the semi-analytic model, for the base and flip versions (dashed and solid lines, respectively). The constraining observational data are shown as different symbols as stated in the key, for the estimates by Norberg et al. (2001) and Jones et al. (2006), both in the b_J band, and from Bell et al. (2003), Cole et al. (2001), Kochanek et al. (2001) and Jones et al. (2006), for the K band. The luminosity functions correspond to two versions of the model run with the same parameters obtained for the base model using the PSO technique (Ruiz et al. 2013). The semi-analytic parameters are given in Section 2.2.

The results for the local galaxy luminosity function in the b_J and K bands, which are used as constrains for the search of the best-fitting parameters, are shown in Fig. 3 for both the base and flip models. The latter is much better able to reproduce the knee of the luminosity functions in comparison to the former. The flip model also provides a better match to the bright end of the luminosity function in both bands, particularly for the K band, even when no additional tuning of parameters was performed.

We now turn to compare the frequency of bursts in the two models, first concentrating on the DI events that affect the star formation activity and lifetime of discs, and then focusing on mergers which induce large flips and therefore allow us to use DIes instead of mass fractions to trigger starbursts.

3 DISC INSTABILITIES

The number of DI in the two calibrated models are found to be different given the tendency towards smaller sizes of discs in the flip model. The upper panel of Fig. 4 shows the number of galaxies that suffered at least one DI event in their lifetimes (excluding instabilities triggered by mergers in the flip model), as a function of stellar mass. The solid line corresponds to the flip model in which, as can be seen, more galaxies suffered bursts of star formation triggered by DIs by even more than two orders of magnitude, more so for lower mass galaxies. The lower panel shows this excess in more detail. Galaxies with high present-day stellar masses have had more instabilities per unit redshift in the flip model at all redshifts, and galaxies with different present-day masses all tend to reach similar maximum average numbers of DIs per unit redshift. In the base model, however, galaxies with low present-day masses suffered very little DIs in comparison with higher present-day mass galaxies. The increase in instabilities in the flips versus the base model becomes more important at lower redshifts, with differences of 2 orders of magnitude or more.

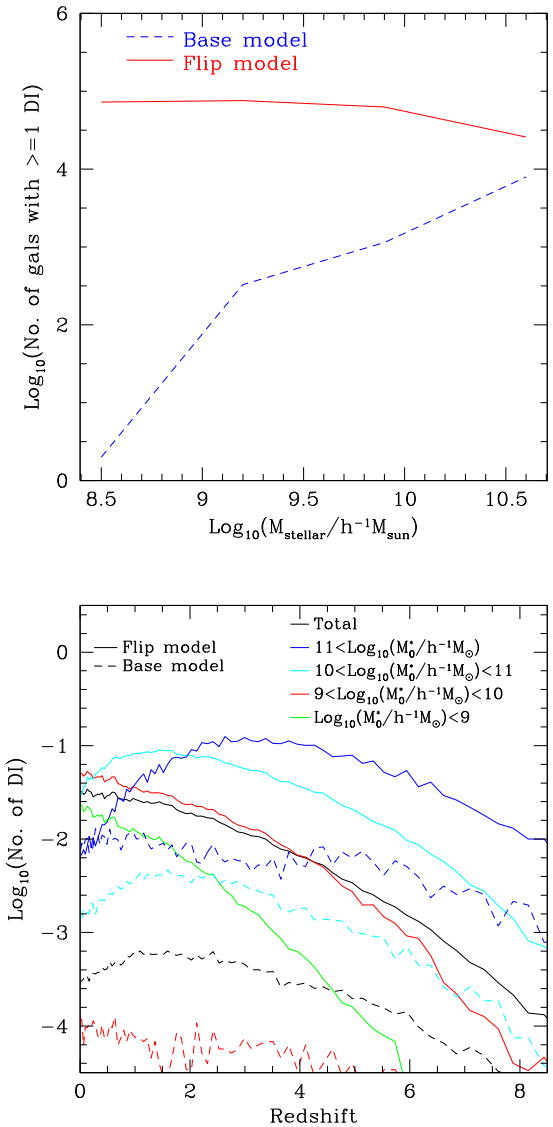

Figure 4. Statistics of the number of DI events in the base and flip models (solid and dashed lines, respectively). Top panel: number of galaxies with at least one DI event in their lifetimes, as a function of stellar mass. Poisson errors are too small to be noticed for the flip model. Bottom panel: number of instabilities per unit redshift suffered by galaxies in different present-day stellar mass ranges and for the total $z = 0$ galaxy population (different colours, as indicated in the key).

The increase in the frequency of DIs which effectively destroy discs translates into different times of disc survivability. We explore these changes in Fig. 5, where the top panel shows the time since the last destruction of a disc by triggered DIs (i.e. not including merger-driven starbursts), as a function of stellar mass. In this case we are showing the median for the full galaxy population, so in some cases there may not actually be discs in the sample, particularly for high stellar mass central galaxies where the AGN feedback is able to prevent a new disc from forming, or for satellite galaxies which do not receive further supply of cool gas. However, in the cases where a disc is present, this time corresponds to the age of the disc that survives to $z = 0$. As can be seen, surviving discs in the flip model show a trend of larger ages for higher stellar masses, ranging from $\sim$3 to $\sim$5 Gyr for galaxies of $M^* = 3 \times 10^8\, h^{-1}\, \mathrm{M}_\odot$ to $M^* = 10^{11}\, h^{-1}\, \mathrm{M}_\odot$, with a large scatter that extends up to $\sim$8 Gyr. The base model shows a similar trend, but surviving discs are roughly a couple of gigayears older than in the flip model, with a slightly larger difference for higher mass galaxies. Notice that in both models discs in small galaxies are relatively young, but discs in massive galaxies are older, as is the case of the Milky Way (e.g. Jimenez et al. 1998; Hopkins et al. 2008; Kazantzidis et al. 2008; Purcell et al. 2008). In particular, both models allow the existence of very old discs for grand-design spiral galaxies.

The lower panel of Fig. 5 shows the average time between consecutive destructions of the disc down to the last burst driven by DIs, i.e. it does not include the last surviving disc of the upper panel. Also, as in the top panel, this statistics does not include merger induced bursts. The base model presents a clear trend, where low-mass galaxies have a higher average time between disc destruction events of 5.5 Gyr to 3.8 Gyr for $M^* = 3 \times 10^8\, h^{-1}\, \mathrm{M}_\odot$ and $M^* = 10^{11}\, h^{-1}\, \mathrm{M}_\odot$, respectively. In the flip model the trend is similar, with a change from 4.3 Gyr to 1.9 Gyr for the same stellar masses, but more importantly, the typical disc lifetime is shorter; discs are more episodic. This is due, in part, to the fact that slews and flips affect more intensely galaxies while they are in a fast growth regime; in this case, the angular momentum flips are more important since the infalling mass is often a large fraction of the previous disc mass. Even galaxies that reached high masses at $z = 0$ went through this stage at some point, and therefore show a lower average disc lifetime than in the base model. In the latter, on the other hand, DIs take more time to occur since only when they reach a critical mass they become unstable. In both models, high-mass galaxies grew in mass during an epoch of faster mass growth (e.g. Lagos, Padilla & Cora 2009b) than lower present-day mass galaxies and, thus, show lower average times between consecutive destructions of the disc.

A possible shortcoming of the flip model is that the fraction of galaxies that have suffered instabilities could have grown to an unacceptable level. However, we find that the increase in frequency of instabilities is present mostly at low stellar masses and high look back times (LBT), as can be seen in Fig. 6. For stellar masses $M_{\mathrm{stellar}} > 10^{11}\, h^{-1}\, \mathrm{M}_\odot$ the flip model shows only about 50 per cent

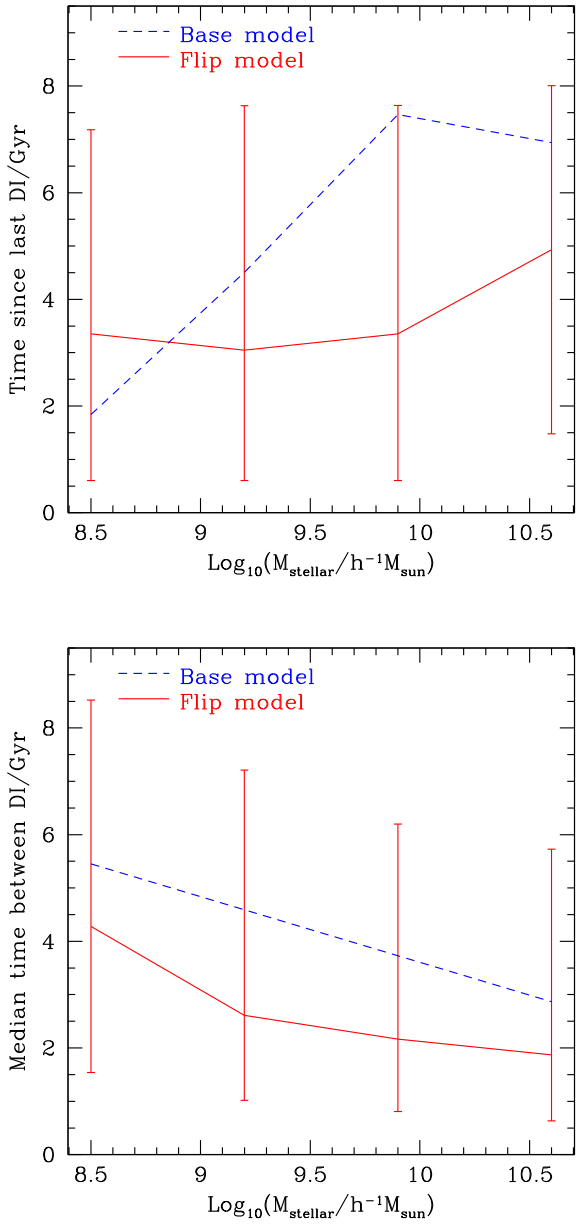

Figure 5. Statistics of disc lifetimes in the base and flip models (dashed and solid lines, respectively). Top panel: time since the last DI event, which can be interpreted as the age of present-day discs, as a function of galaxy stellar mass. Bottom: median time between consecutive DIs, which effectively represents the typical lifetime of discs previous to the surviving disc (whose age is represented in the top panel), for galaxies that have suffered at least one DI. Error bars correspond to the 20 and 80 percentiles of the distribution, shown only for the flip model for clarity.

more instabilities per galaxy than the base model for LBT <3 Gyr. For the same mass range, for LBT<5 and 7 Gyr, the flip model shows about twice as many instabilities as the base model. Notice that a LBT of 3 Gyr is about one order of magnitude longer than a typical dynamical time, and therefore present day massive galaxies should show signs of a recent DI in only ∼10–15 per cent of the cases, for both models. The main difference is that in the flip model, this percentage remains roughly constant with stellar mass down to $M_{\rm stellar} = 10^8\,h^{-1}\,{\rm M}_{\odot}$.

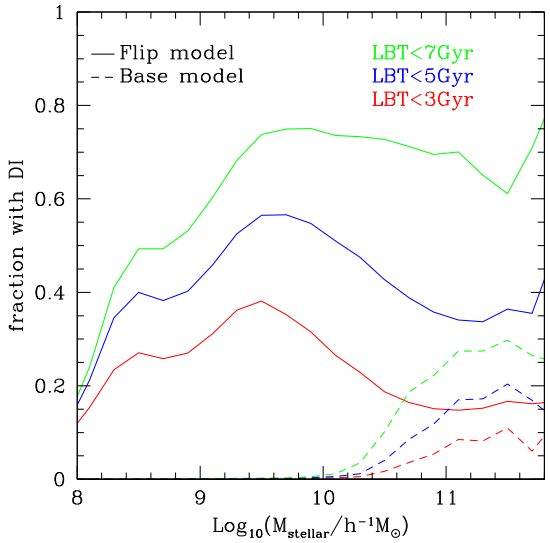

Figure 6. Fraction of galaxies that have suffered at least one DI in the last 3, 5, and 7 gigayears (red, blue and green lines, respectively), as a function of stellar mass, for the base and flip models (dashed and solid lines, respectively).

4 DISC INSTABILITY DRIVEN STARBURSTS IN MERGERS

As was mentioned in Section 2, in the flip model we do not make use of mass ratios to decide whether a galaxy that has just undergone a merger suffers a burst of star formation; rather we simply check whether the disc of the remnant galaxy is stable or not.

As the actual mergers of galaxies are governed by the merger trees extracted from the numerical simulation, both versions, the base and flip models, will have the same total number of mergers between galaxies. However, since the evolution of the baryons in each model is different, the fraction of mergers with baryonic mass ratios above a given threshold can be different. Furthermore, the conditions for the triggering of bursts are completely different between the models, and therefore the number of mergers with starbursts is also not expected to be the same.

In the base model, the parameters that are used to decide whether there is a burst in a merger are (i) $f_{\rm major} = 0.3$, the mass ratio that defines a major merger such that if two colliding galaxies are characterized by a higher mass ratio, all the cold gas will be turned into stars and sent to the bulge, along with any other stars in the discs of the merging galaxies; since in rare cases there will be no cold gas in the colliding galaxies, the fraction $f_{\rm gas,\ major} = 0.6$ is used to define the major merger as dry or wet, depending on whether the fraction of gas in the disc of the accreted satellite is below or above this threshold (Jiménez et al. 2011); notice, however, that $f_{\rm gas,\ major}$ is not a parameter of the model as it does not affect the evolution of the galaxies. (ii) $f_{\rm disc,\ burst} = 0.6$ is the fraction of gas in the larger of the galaxies involved in a minor merger (i.e. with a mass ratio lower than $f_{\rm major}$), above which there will be a burst that will transform all the available cold gas into stars and add them to the bulge, with the stars in the disc left untouched in this case, and (iii) $f_{\rm burst} = 0.05$, the minimum mass ratio for the $f_{\rm disc,\ burst}$ condition to take place; if this is not satisfied, there is no burst. The flip model drops three of the parameters of the base model by simply producing a burst if the disc of the remnant galaxy is unstable, considering the merger itself sufficient enough for a perturbation to trigger the instability. This

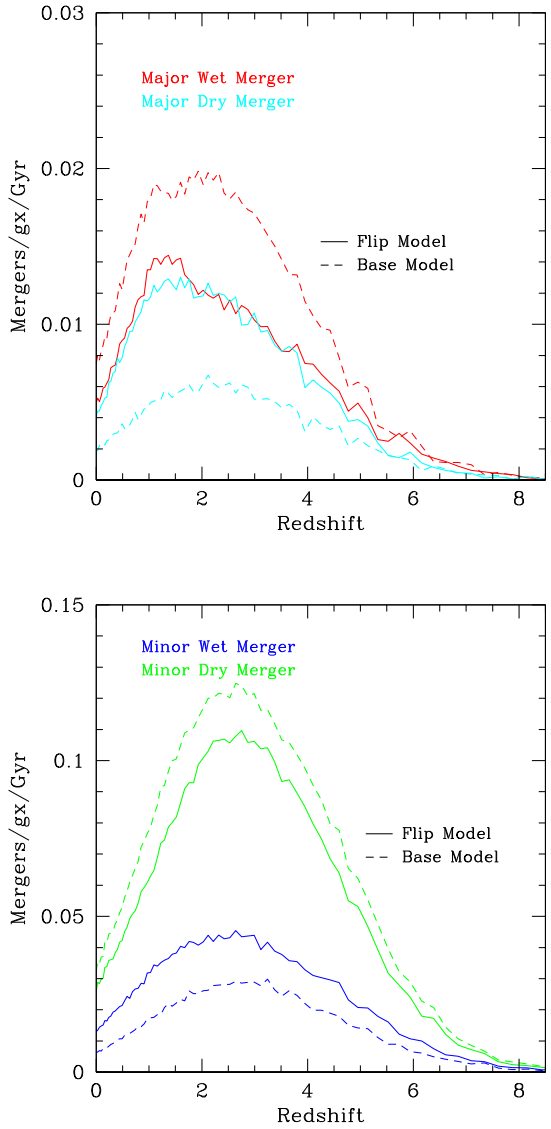

Figure 7. Frequency of mergers per galaxy per gigayear, separated into events with different mass ratios between the merging galaxies corresponding to major (mass ratios >0.3, top panel) and minor (bottom) mergers. The flip and base models are represented by solid and dashed lines, respectively. Different colours denote wet and dry mergers (see the figure key), where the former correspond to events where a starburst was triggered, whereas the latter refer to mergers with no ensuing star formation.

way the flip model greatly diminishes the parameter space freedom typical of semi-analytic models.

We compare the frequency of mergers either with or without a starburst in the base and flip models in Fig. 7. We separate the statistics in major and minor mergers according to the ratio of the masses of the merging galaxies and show the results in the upper and lower panels of the figure, respectively, for the flip and base models (solid and dashed lines, respectively). The colours help distinguish between dry and wet mergers. In the latter type of merger a starburst takes place, whereas in dry mergers there is no immediate star formation as a result of the merger. The exception to this rule are dry major mergers in the base model which correspond to the case when the satellite cold gas mass fraction is below $f_{\rm gas,\,major}$.

As can be seen, given that the merger trees extracted from the numerical simulation set the total frequency of mergers, the overall merger rates in both models appear similar at first sight. However, there are important differences between them. The flip model presents a larger quantity of dry major mergers, by about a factor of 2 compared to the base model. Given that a major merger produces an important flip in the angular momentum of a galaxy disc, and therefore impedes the growth of the size of the galaxy, the fact that there are no bursts in these cases is an indication that the remnant galaxy is not massive enough to become unstable and thus trigger a starburst. In the base model, any available gas will undergo a burst. However, as was shown in the previous section, in the flip model the frequency of DIs is much higher than in the base model, which acts to balance the offset in merger-driven starbursts in the model, causing little difference to the galaxy colours and to the morphological fractions as a function of stellar mass, for instance (cf. following section and Fig. 9).

In the case of minor mergers, the results are very similar between the two models, with only a 15 per cent deficit (increment) of dry (wet) minor mergers in the flip with respect to the base model. Another difference with respect to the major merger case is then that this slight excess of minor wet mergers is not counteracted by the bursts driven by DIs (cf. the previous section), since both effects go in the same direction of having more bursts when the accretion of baryonic matter carries small amounts of matter.

In the following sections we will then use the flip model with DIs as the only driver of starbursts in galaxies, both in perturbed galaxies and in the remnant galaxies of mergers, bearing in mind the possible influence of more frequent bursts in smooth accretion events and minor mergers.

5 TESTABLE CONSEQUENCES

Even though the $z = 0$ galaxy populations in the base and flip models show similar luminosity functions (Fig. 3), it is clear that there are differences in other galaxy properties. In this section we show some of these differences and make further comparisons to observational data, when available.

Our first comparison is focused on the dimensionless spin parameter of galaxies. Cervantes-Sodi et al. (2008) measured this quantity for a sample of galaxies taken from the Sloan Digital Sky Survey (SDSS; York et al. 2000) using a simple model for their dynamical structure. Fig. 8 shows their results compared to our models. As can be seen, when assuming the spin of the galaxy to coincide with that of the disc, then both models provide similar agreement, but without the trend of higher spins for lower stellar masses. The flip model shows slightly lower spins due to the effect of the slews and flips.

The change in the frequency of DIs, and the mechanism to trigger starbursts in general, can cause the morphological fractions to vary between the base and flip models. Therefore, we compare the $z = 0$ fractions of galaxies with different morphologies as a function of their stellar mass in Fig. 9. Model galaxies are separated into different morphological classes according to their bulge to total stellar mass ratios. Irregular galaxies are those with no bulge,[2] spirals contain a bulge which can make up for up to 80 per cent of the total stellar mass, and ellipticals contain more than 80 per cent of their stellar mass in a bulge. Since the total population of galaxies is divided into one of these three types, we only show the results for irregular and elliptical galaxies. As can be seen, the base model shows good agreement for the elliptical and irregular

[2] The results of Fig. 9 do not change significantly when changing the upper limit in bulge-to-total stellar mass ratio for irregulars from 0 to 5 per cent.

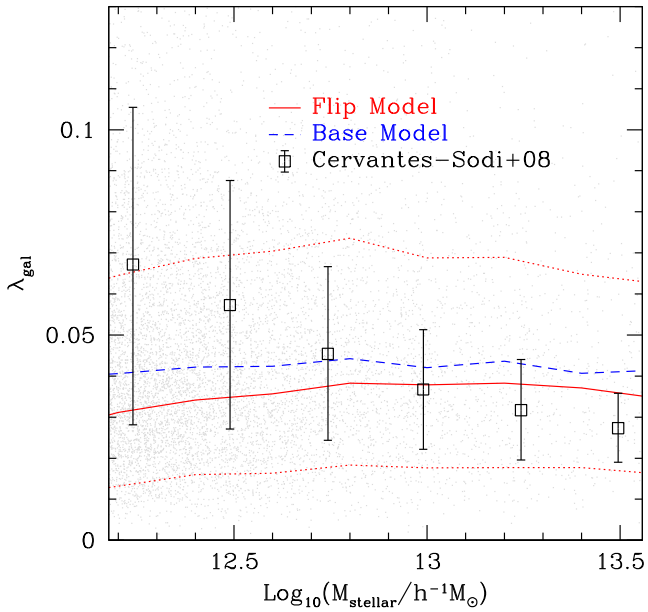

Figure 8. Dimensionless spin parameter of galaxies as a function of their host dark-matter halo mass. The open squares with error bars correspond to measurements for SDSS galaxies by Cervantes-Sodi et al. (2008). The grey points show the scatter of galaxy spins in the flip model; the solid red line corresponds to the median of these points and the dotted lines show the 10 and 90 percentiles. The blue dashed line shows the median of the base model.

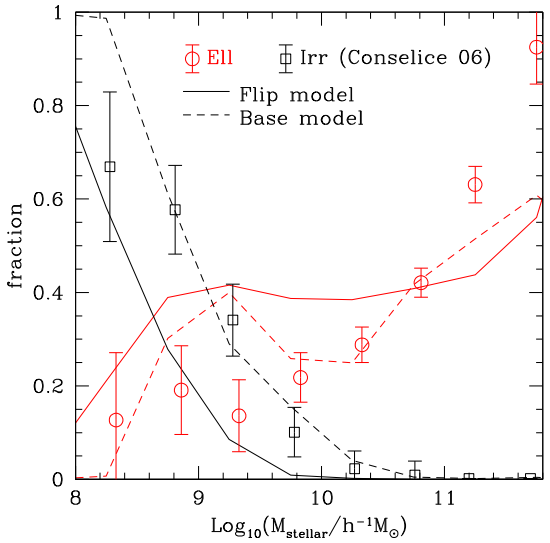

Figure 9. Fractions of galaxies with elliptical and irregular morphology (red and black, respectively), as a function of stellar mass, for the base (dashed lines) and flip (solid lines) models. The symbols with error bars show the results for nearby galaxies obtained by Conselice (2006) for the same galaxy types.

galaxies, with only a slight excess of ellipticals around $M_{\rm stellar} = 10^9\,h^{-1}\,{\rm M}_\odot$ and of irregulars at $M_{\rm stellar} = 10^8\,h^{-1}\,{\rm M}_\odot$. In the case of the flip model, the higher frequency of DIs is responsible for a drop in the frequency of galaxies with no bulge, which is only slightly at odds with the data and at the lowest stellar masses the agreement improves. The flip model shows reasonable agreement with the observed fraction of elliptical galaxies, although slightly less so than the base model. Notice though that the flip model

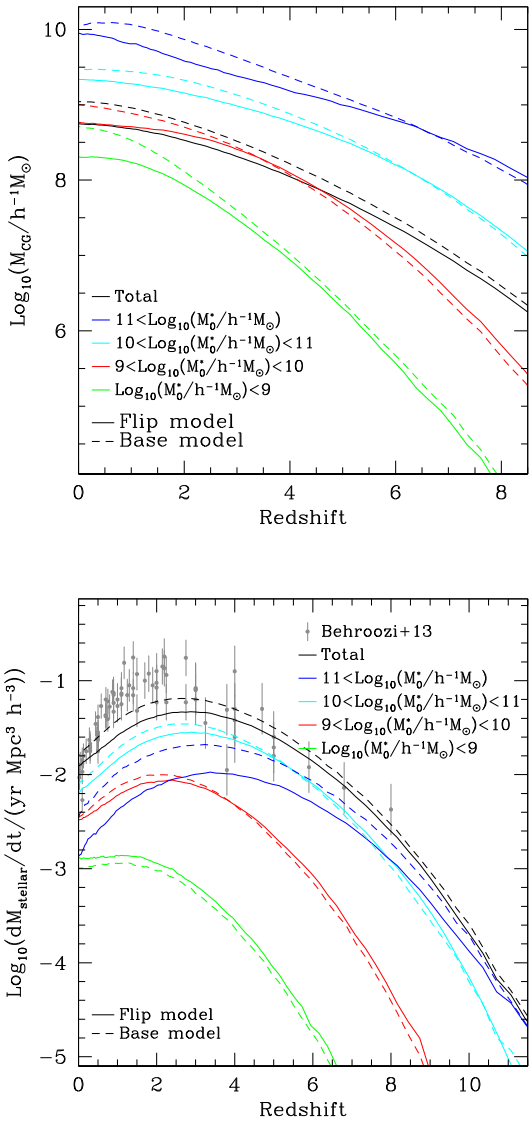

Figure 10. Top panel: cold gas mass for all the $z = 0$ galaxies in each model (black) and different present-day stellar mass ranges (colours, see the figure key), for the base and flip models (dashed and solid lines, respectively). Bottom: star formation rate density as a function of redshift for the full $z = 0$ galaxy population (black) and different present-day stellar mass ranges for the base and flip models (same colours and line types as top panel). The grey points with error bars correspond to the observational compilation by Behroozi, Wechsler & Conroy (2013).

parameters were not recalibrated to fit any observables, and the agreement which is already reasonable could improve further with a slightly different set of parameters. Also, we remind the reader that the flip model does qualitatively improve the agreement with the knee and bright end of the luminosity functions (cf. Fig. 3); these tests simply show that it also provides a reasonable frequency of bulges.

Fig. 10 shows a comparison of the cold gas mass and star formation rate density as a function of redshift (top and bottom panels, respectively) resulting from the two models, for the full galaxy population and for galaxies with different present-day stellar masses, as indicated in the figure key. The star formation rate densities of the models are further compared to the data compiled by Behroozi et al. (2013). The model star formation rate densities were divided by

1.515 to convert them to the Chabrier initial mass function adopted by Behroozi et al. In both panels, the solid lines represent the flip model, whereas the dashed lines correspond to the base model. As expected, due to the lower star formation activity in the latter, the amount of cold gas in galaxies is higher in the base model, particularly at low redshifts; the flip model spends more cold gas as a result of the slower growth of angular momentum due to the action of the slews and flips. In terms of the full galaxy population, the different models differ in this quantity by about a factor of 2 at $z = 0$.

The lower panel of the figure shows that at high redshifts the star formation rate density tends to be higher in the flip model, except for the most massive galaxies. Then, at lower redshifts for lower final stellar mass galaxies, the star formation rate densities of the two models equal each other until the base model starts to show higher rates. For instance, this transition occurs at $z \sim 4$ for $10^9\,h^{-1}\,\mathrm{M}_\odot < M^* < 10^{10}\,h^{-1}\,\mathrm{M}_\odot$, and at $z \sim 5.5$ for $10^{10}\,h^{-1}\,\mathrm{M}_\odot < M^* < 10^{11}\,h^{-1}\,\mathrm{M}_\odot$, whereas for $M^* < 10^9\,h^{-1}\,\mathrm{M}_\odot$ the star formation activity is still higher for the flip model at $z = 0$. This effectively shows that the flip model is downsizing more effectively than the base model. The grey symbols represent the compilation of observational results by Behroozi et al. (2013). As can be seen, the scatter in the observations is similar to that present between the base and flip models, making both of them roughly consistent with the observations.

An immediate consequence of having a higher star formation rate at high redshifts is that the stellar mass in galaxies grows at a faster rate. Therefore an interesting comparison with observations is the one that focuses on the stellar mass function which, at high redshifts, has been difficult to reproduce by semi-analytic models (e.g. de Lucia et al. 2006), as was mentioned in the Introduction. Fig. 11 shows the stellar mass function for galaxies at $z = 3.5$ extracted from the base and flip models (dashed and solid lines, respectively). As expected, the flip model produces more high stellar mass galaxies, with a general shift of the stellar mass function towards higher masses by 20 per cent. This increase shortens the gap between the flip model stellar masses and the estimates from the NEWFIRM medium band survey by Marchesini et al. (2010) for massive galaxies at $3 < z < 4$, particularly for the case when they consider dusty templates to fit their observed photometry. In their paper, Marchesini et al. show that this mass function would only be consistent with the Somerville et al. (2008) galaxies if they included a 0.25 dex error in the mass estimates for the model galaxies. In the flip model case, a 0.25 dex error (dotted line) makes the stellar mass function agree with the dusty–template case in Marchesini et al.

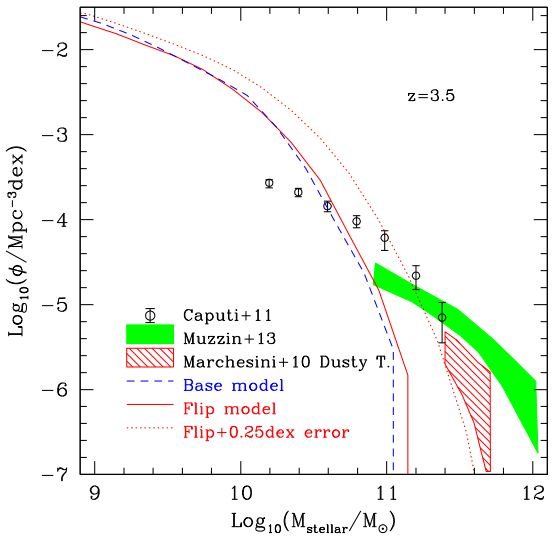

Figure 11. Stellar mass functions for model galaxies at $z = 3.5$ for the base and flip models (dashed and solid lines, respectively). The dotted line shows the results for the flip model if a Gaussian error of width 0.25 dex in the logarithm of the stellar mass is added to the model masses. The shaded regions correspond to the NEWFIRM medium band survey sample of massive galaxies at $3 < z < 4$, when adopting the dusty template set (Marchesini et al. 2010), and the results for the ULTRAVISTA survey (McCracken et al. 2012) by Muzzin et al. (2013), whereas the symbols show the results by Caputi et al. (2011) for the UDS, as indicated in the key.

The figure also shows a lack of agreement between the flip model and the Muzzin et al. (2013) data at the high-mass end of the stellar mass function, but it should be taken into consideration that they did not include a dusty template as was done by Marchesini et al. In their appendix, Muzzin et al. state that the number density of the most massive galaxies diminishes considerably when they add this template to their set which would improve our agreement with their results. Notice also that the number density of dwarf galaxies with $M_\star < 10^{10}\,h^{-1}\,\mathrm{M}_\odot$ does not change between the two flavours of this model implying that even though the formalism adopted in the flip model increases the stellar mass growth at high redshifts, it does not do so at the expense of a larger population of dwarf galaxies (cf. Henriques et al. 2013). The dwarfs with stellar masses around the $10^{10}\,h^{-1}\,\mathrm{M}_\odot$ mark in our model appear to be over-abundant in comparison to the results by Caputi et al. (2011) for the UDS (Williams et al. 2009). Notice, however, that Caputi et al. also do not include dusty templates as Marchesini et al.

Given the changes to the galaxy sizes imprinted by the inhibition of angular momentum growth due to flips, it is also necessary to study the distributions of galaxy sizes in the new model. In principle, one can think that inhibiting the growth of the angular momentum would result in smaller disc sizes. However, when measuring the median size of surviving spiral galaxies at $z = 0$ and $z = 4$ in the upper and lower panels of Fig. 12, respectively, we see that this is the case, but to a small extent. At $z = 0$, the flip model shows similar median galaxy sizes than the base model almost throughout the entire range of magnitudes shown, and both models are in similar agreement with SDSS galaxy sizes measured by González et al. (2009). As was shown by Bruce et al. (2012), the spiral disc sizes at $z = 2$ are quite similar to those of $z = 0$, and therefore we go to higher redshifts for our next comparison. We use the recent measurement of $z = 4$ Lyman-Break Galaxies (LBGs) with sizes estimated from CANDELS (Wuyts et al. 2011) data by Huang et al. (2013). In this case, the base model shows sizes consistent with the observed ones, and this is also the case for the flip model, except at the bright end where flip model galaxies flatten their size and become slightly (25 per cent) smaller than the observed ones.

The reason for the similar sizes between the two models at all redshifts is that the flip model first tends to distort the distribution of galaxy sizes by extending a tail towards small disc radii, but at the same time the DI mechanism quickly destroys the smaller discs, making this distribution lose its small radii tail and, consequently, show a similar median value to that of the base model. This effect is present at all luminosities at both redshift ranges.

6 CONCLUSIONS

In this work we presented the implementation of angular momentum slews and flips in a semi-analytic galaxy formation model. The aim in doing this was to reproduce in a more realistic way the fact that often the angular momentum of discs and that of the matter they

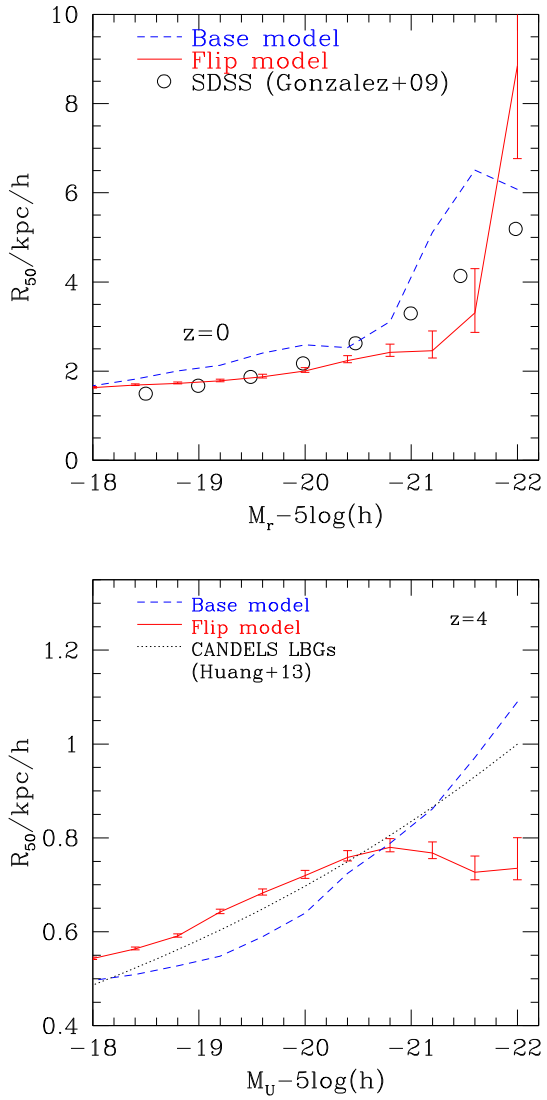

Figure 12. Galaxy radii containing 50 per cent of the total flux, as a function of absolute magnitude, for the base and flip models (dashed and solid lines, respectively). Top panel: $z = 0$ results for spirals, as a function of r-band absolute magnitude, compared to results from the Sloan Digital Sky Survey Main Galaxy Sample from González et al. (2009). Bottom: $z = 4$ sizes of star-forming galaxies in the models, and Lyman Break Galaxies (dotted lines; Huang et al. 2013) from the CANDELS survey (Wuyts et al. 2011). The error bars are shown only for the flip model, and indicate the error on the mean.

accrete are not aligned. This lack of alignment is thought to be responsible for the destruction of discs within dark-matter haloes that do not necessarily undergo a dramatic event such as a merger. The interaction of the infalling material with the disc as it arrives makes the discs to become unstable, undergo bursts, and feed new stars to a bulge.

From the hydrodynamical side, Sales et al. (2012) used the GIMIC galaxies to show that most of the discs that survive at $z = 0$ show angular momentum vectors that are better aligned with the matter at turn around than particles in a spheroid component. This indicates that misaligned infall could be responsible for the formation of bulges. A possible reason behind this is that the dark-matter halo that hosts a galaxy suffers several stochastic changes in its angular momentum vector as shown by Bett & Frenk (2012). If the hot gas that cools towards the disc is relaxed in this dark-matter halo, in most cases the cooling gas will have an angular momentum that will not necessarily be parallel to that of the cold disc it is destined to feed.

In most semi-analytic models, the resolution of the parent dark-matter simulation does not allow for the direction of the angular momentum of the halo to be measured with high accuracy. For this, at least 1000 particles per halo are needed, and most semi-analytic models use haloes with of the order of 10 or more particles. Therefore, we measured the probability of angular momentum flips by a given angle using subhaloes of the Millennium II simulation (Boylan-Kolchin et al. 2009) after they change their mass by a certain relative amount, in different redshift ranges. We construct different probability distributions for when the accretion is smooth or due to mergers. In particular, we find that at high redshifts the same relative increase in mass produces larger flips in the angular momentum of haloes. This is also the case for mergers in comparison to smooth accretion.

We apply flips to the semi-analytic model SAG (Cora 2006; Lagos et al. 2008, 2009a; Tecce et al. 2010) by using Monte Carlo simulations for the flips suffered by the galaxy angular momenta. To do this, we assume that the distributions of flips measured in the subhaloes apply as well to the baryons at their centres and that, in addition, their effect is that of slowing down the growth of angular momentum of discs with respect to their host haloes. The motivation behind this assumption comes from the results of hydrodynamical simulations that show that infalling material with misaligned angular momenta with respect to the galaxy disc could be responsible for its repeated destruction (Sales et al. 2012; Aumer et al. 2013). In our new implementation, the net effect of the flips is that the average disc slows down its angular momentum acquisition during its most active growth phase to then continue growing at later times. The discs that are more affected by this are those which accrete mass with misaligned angular momentum, and are those more prone to undergo instabilities and to be added to their bulge.

Even though discs are more unstable in the flip model, the galaxies that reach high present-day stellar masses have not been subject to DIs in just as long a time as in a model with no flips, i.e. grand-design spiral discs are also old in the flip model. However, the past history of these galaxies includes shorter lived previous incarnations of discs, i.e. more episodic discs, since the flips are more important while a galaxy is still small as it is growing in size in larger relative fractions of its mass compared to higher mass galaxies.

As the inclusion of flips increases the star formation activity at high redshifts, the stellar mass function of high redshift galaxies reaches slightly higher masses, slightly improving the agreement with observations at high redshift.

We also take advantage of the large flips suffered by galaxies during mergers to use the DI condition to produce bursts in mergers. This way our model reduces its parameter space, dispensing of three parameters that, in the base model, are used to determine whether there are bursts via conditions on different mass ratios of the merging galaxies. The resulting fractions of wet mergers (i.e. with bursts of star formation) in the flip model are reduced compared to the base model, but the higher frequency of bursts due to other DI events in the former compensates for this and makes a final galaxy population that is similar in the two models in terms of colours and morphologies.

Massive galaxies in the flip model form stars more rapidly at early times, and have less available cold gas for star formation at later times providing a better fit to the steep fall off of the bright end of the luminosity function.

ACKNOWLEDGEMENTS

This work was supported in part by Fondecyt Regular No. 1110328, BASAL PFB-06 'Centro de Astronomia y Tecnologias Afines'. NP and SC acknowledge support by the European Commissions Framework Programme 7, through the Marie Curie International Research Staff Exchange Scheme LACEGAL (PIRSES-GA-2010-269264). We have benefitted from fruitful discussions with Yuval Birnboim, David Wilman, Bruno Henriques, Francoise Combes, Laura Sales, Noam Libeskind, Simon White and Carlos Frenk. We thank the anonymous referee for helpful comments. NP thanks the hospitality of the Max Planck Institute for Astrophysics at Garching, where part of this work was done and several helpful discussions were held. The Geryon cluster at the Centro de Astro-Ingenieria UC was extensively used for the calculations performed in this paper. The Anillo ACT-86, FONDEQUIP AIC-57, and QUIMAL 130008 provided funding for several improvements to the Geryon cluster. This work was partially supported by the Consejo Nacional de Investigaciones Científicas y Técnicas (CONICET, Argentina), Secretaría de Ciencia y Tecnología de la Universidad Nacional de Córdoba (SeCyT-UNC, Argentina), Universidad Nacional de La Plata (UNLP, Argentina), and Instituto de Astrofísica de La Plata (IALP, Argentina). SAC acknowledges grants from CONICET (PIP-220), Argentina, Agencia Nacional de Promoción Científica y Tecnológica (PICT-2008-0627), Argentina, and Fondecyt No. 1110328, Chile. The Millennium II Simulation data base used in this paper and the web application providing online access to them were constructed as part of the activities of the German Astrophysical Virtual Observatory (GAVO).

REFERENCES

Algorry D., Navarro J., Abadi M., Sales L., Steinmetz M., Piontek F., 2014, MNRAS 437, 3596
Aumer M., White S., Naab T., Scannapieco C., 2013, MNRAS 434, 3142
Baugh C., 2006, Rep. Progress Phys., 69, 3101
Behroozi P., Wechsler R., Conroy C., 2013, ApJ, 770, 57
Bell E., McIntosh D., Katz N., Weinberg M., 2003, ApJS, 149, 289
Benson A., 2010, Phys. Rev., 495, 33
Berry M., Somerville R., Haas M., Gawiser E., Maller A., Popping G., Trager S., 2014, MNRAS 441, 939
Bett P., Frenk C., 2012, MNRAS, 420, 3324
Bird J., Kazantzidis S., Weinberg D., Guedes J., Callegari S., Mayer L., Madau P., 2013, ApJ, 773, 438
Bois M. et al., 2011, MNRAS, 416, 1654
Bower R., Benson A., Crain R., 2012, MNRAS, 422, 2816
Boylan-Kolchin M., Springel V., White S., Jenkins A., Lemson G., 2009, MNRAS, 398, 1150
Brook C. B. et al., 2011, MNRAS, 415, 1051
Bruce V. et al., 2012, MNRAS, 427, 1666
Bullock J., Kolatt T. S., Sigad Y., Somerville R. S., Kravtsov A. V., Klypin A. A., Primack J. R., Dekel A, 2001, MNRAS, 321, 559
Caputi K. I., Cirasuolo M., Dunlop J. S., McLure R. J., Farrah D., Almaini O., 2011, MNRAS, 413, 162
Cervantes-Sodi B., Hernandez X., Park C., Kim J., 2008, MNRAS, 388, 863
Cole S., Lacey C., Baugh C., Frenk C., 2000, MNRAS, 319, 168
Cole S. et al., 2001, MNRAS, 326, 255
Conselice J. C., 2006, MNRAS, 373, 1389
Cora S., 2006, MNRAS, 368, 1540
Crain R. et al., 2009, MNRAS, 399, 1773
Croton D. et al., 2006, MNRAS, 367, 864
D'Onghia E., Burkert A., 2004, ApJ, 612, 13
De Lucia G., Springel V., White S., Croton D., Kauffmann G., 2006, MNRAS, 366, 499
Dubinski J., Chakrabarty D., 2009, ApJ, 703, 2068
Dutton A., van den Bosch F., 2012, MNRAS, 421, 608
Ferreras I., Lisker T., Pasquali A., Khochfar S., Kaviraj S., 2009, MNRAS, 396, 1573
Garcia-Ruiz I., Kuijken K., Dubinski J., 2002, MNRAS, 337, 459
González J., Lacey C., Baugh C., Frenk C., Benson A., 2009, MNRAS, 397, 1254
Guedes J., Callegari S., Madau P., Mayer L., 2011, ApJ, 742, 438
Guo X. et al., 2011, MNRAS, 413, 101
Henriques B., White S., Thomas P., Angulo R., Guo Q., Lemson G., Springel V., 2013, MNRAS, 431, 3373
Hopkins P., Hernquist L., Cox T. J., Younger J. D., Besla G., 2008, ApJ, 688, 757
Hopkins P. F., Quataert E., Murray N., 2011, MNRAS, 417, 950
Huang K.-H., Ferguson H., Ravindranath S., Su J., 2013, ApJ, 765, 68
Jarosik N. et al., 2011, ApJS, 192, 14
Jimenez R., Flynn C., Kotoneva E., 1998, MNRAS, 299, 515
Jiménez N., Cora S., Bassino L., Tecce T., Smith Castelli A., 2011, MNRAS, 417, 785
Jones D., Peterson B., Colless M., Saunders W., 2006, MNRAS, 369, 25
Kannan R., Stinson G. S., Maccio A. V., Brook C., Weinmann S. M., Wadsley J., Couchman H. M. P., 2014, MNRAS, 437, 3529
Kauffmann G., Colberg J., Diaferio A., White S., 1999, MNRAS, 303, 188
Kazantzidis S., Bullock J. S., Zentner A. R., Kravtsov A. V., Moustakas L. A., 2008, ApJ, 688, 254
Kennicutt R., 1998, ApJ, 498, 541
Kochanek C. et al., 2001, ApJ, 560, 566
Lagos C., Cora S., Padilla N., 2008, MNRAS, 388, 587
Lagos C., Padilla N., Cora S., 2009a, MNRAS, 395, 625
Lagos C., Padilla N., Cora S., 2009b, MNRAS, 397, 31L
Lagos C. D. P., Padilla N., Strauss M., Cora S., Hao L., 2011, MNRAS, 414, 2148
Lemson G., The Virgo Consortium, 2006, preprint (astro-ph/0608019)
McCracken H. J. et al., 2012, A&A, 544, A156
Maller A., Dekel A., 2002, MNRAS, 335, 487
Marchesini D. et al., 2010, ApJ, 725, 1277
Marinacci F., Pakmor R., Springel V., 2014, MNRAS, 437, 1750
Mo H., Mao S., White S., 1998, MNRAS, 295, 319
Muzzin A. et al., 2013, ApJ, 777, id 18
Naab T. et al., 2013, MNRAS (arXiv:1311.0284)
Nagamine K., 2010, Adv. Astron., 2010
Norberg P. et al., 2001, MNRAS, 328, 64
Pérez-González P. et al., 2008, ApJ, 675, 234
Powell L., Slyz A., Devriendt J., 2011, MNRAS, 414, 3671
Purcell C., Kazantzidis S., Bullock J. S., 2008, ApJ, 694, L98
Robertson B., Bullock J., Cox T., Di Matteo T., Hernquist L., Springel V., Yoshida N., 2006, ApJ, 645, 986
Romanowsky A., Fall M., 2012, ApJS, 203, 17
Ruiz A. et al., 2013, MNRAS (arXiv:1310.7034)
Saha K., Naab T., 2013, MNRAS, 434, 1287
Sales L., Navarro J., Theuns T., Schaye J., White S., Frenk C., Crain R., Dalla Vecchia C., 2012, MNRAS, 423, 1544
Scannapieco C., Tissera P., White S., Springel V., 2006, MNRAS, 371, 1125
Scannapieco C. et al., 2012, MNRAS, 423, 1726
Shen J., Sellwood J. A., 2006, MNRAS, 370, 2
Silk J., Mammon G., 2012, Res. Astron. Astrophys., 12, 917
Somerville R., Hopkins P., Cox T., Robertson B., Hernquist L., 2008, MNRAS, 391, 481
Springel V., 2005, MNRAS, 364, 1105
Springel V., 2010, MNRAS, 41, 791
Springel V. et al., 2005, Nature, 435, 629
Springel V. et al., 2008, MNRAS, 391, 1685

Springel V., White S. D. M., Tormen G., Kauffmann G., 2001, MNRAS, 328, 726
Stewart K., Brooks A., Bullock J., Maller A., Diemand J., Wadsley J., Moustakas L., 2013, ApJ, 769, 74
Tasker E. J., 2011, ApJ, 730, 11
Tecce T., Cora S., Tissera P., Abadi M., Lagos C., 2010, MNRAS, 408, 2008
Vitvitska M., Klypin A., Kravtsov A., Wechsler R., Primack J., Bullock J., 2002, ApJ, 581, 799
Williams R. J., Quadri R. F., Franx M., van Dokkum P., Labbé I., 2009, ApJ, 691, 1879
Wuyts S. et al., 2011, ApJ, 742, 96
York D. et al., 2000, AJ, 120, 1579

This paper has been typeset from a TEX/LATEX file prepared by the author.